Surfactant-Assisted Synthesis of the SBA-8 Mesoporous Silica by Using Nonrigid Commercial Alkyltrimethyl Ammonium Surfactants

Jamal El Haskouri,[†] Saúl Cabrera,[‡] Maite Caldés,[§] Carmen Guillem,[†] Julio Latorre,[†] Aurelio Beltrán,[†] Daniel Beltrán,[†] M. Dolores Marcos,*[,||] and Pedro Amorós*[,†]

Institut de Ciència dels Materials de la Universitat de València (ICMUV), P.O. Box 2085, 46071 Valencia, Spain, Laboratorio de Sólidos y Química Teórica, Instituto de Investigaciones Químicas UMSA, Cota-Cota, Calle no. 27, La Paz, Bolivia, Institut des Materiaux Jean Rouxel, Laboratoire de Chimie des Solides, UMR CNRS 110, Université de Nantes, P.O. Box 32229, 44322 Nantes Cedex, France, and Departamento de Química, Universidad Politécnica de Valencia, Camino de Vera s/n, 46071 Valencia, Spain

Received December 14, 2001. Revised Manuscript Received March 25, 2002

A new simple method for obtaining the intermediate ribbonlike SBA-8 mesoporous silica is presented and discussed. We show how the SBA-8 phase can be prepared with the help of commercial alkyltrimethylammonium nonrigid surfactants (such as cetyltrimethylammonium bromide) instead of rigid bolaform amphiphiles, which were used as templates in the only SBA-8 synthesis procedure previously reported. The method is based on the use of atrane complexes as silicon precursors, and we also show how bringing into play fundamental kinetic parameters (like reaction time and temperature at which the successive reaction steps are carried out) makes it possible to modulate the resulting material topology.

Introduction

The discovery of the silica-based FSM-16[1] and M41S[2] mesostructured/mesoporous derivatives brought about the beginning of a new age in the porous materials chemistry. Since then, a great effort has been devoted to the characterization of new mesoporous materials because of their real and potential applications.[3] The Mobil scientists report on the use of cationic alkyltrimethylammonium surfactants as supramolecular templates (or structural directing agents) in the synthesis of the M41S silica family,[2] which was key to further success in this field. In fact, most of the currently known mesoporous silicas and related materials have been synthesized under this approach, making use of these or alternative surfactants or supramolecular templates. Indeed, anionic and nonionic surfactants as well as other amphiphilic molecules (like block copolymers) have been successfully used to prepare new mesoporous silicas. Some of the latter are ordered phases, such as SBA-*n* (n = 1, 2, 3, and 8)[4−8] (prepared with gemini, bolaform, or large headgroup surfactants) and SBA-*n* (n = 11−16)[9] (prepared using block copolymers as templates). Also, disordered mesophases, like HMS, MSU-*n* ,and MSU−V,[10−12] have been synthesized using nonionic surfactants. Other approaches that mimic the FSM-16 synthesis[1] involve the presence of preformed lamellar inorganic precursors (such as the kanemite used in the synthesis of KSW-2 materials).[13]

Insofar as surfactants or supramolecular templates act as structural directing agents, it does not seem surprising that mesostructured/mesoporous silicas display topologies closely related to those observed for the liquid-crystal-like phases typical of surfactant−water systems. In other words, the structural evolution observed in the case of the silica mesophases is clearly reminiscent of that characteristic of the liquid-crystal phases as a function of the surfactant concentration. In short, such a characteristic evolution with the surfactant concentration is cubic (discontinuous phases), hexago-

* To whom correspondence should be addressed. P. Amorós: phone, +34-96-3983617; fax, +34-96-3983633; e-mail, pedro.amoros@uv.es. M. D. Marcos: e-mail, mmarcos@upvnet.upv.es.
[†] ICMUV.
[‡] Instituto de Investigaciones Químicas UMSA.
[§] Université de Nantes.
[||] Universidad Politécnica de Valencia.

(1) Yanagisawa, T.; Shimizu, T.; Kuroda, K.; Kato, C. *Bull. Chem. Soc. Jpn.* **1990**, *63*, 988.
(2) Kresge, C. T.; Leonowicz, M. E.; Roth, W. J.; Vartuli, J. C.; Beck, J. S. *Nature* **1992**, *359*, 710.
(3) Ying, J. Y.; Mehnert, C. P.; Wong, M. S. *Angew. Chem., Int. Ed.* **1999**, *38*, 56.
(4) Huo, Q.; Margolese, D. I.; Cielsa, U.; Feng, P.; Gier, T. E.; Sieger, P.; Leon, R.; Petroff, P. M.; Schüth, F.; Stucky, G. D. *Nature* **1994**, *368*, 317.
(5) Monnier, A.; Schüth, F.; Huo, Q.; Kumar, D.; Margolese, D. I.; Maxwell, R. S.; Stucky, G. D.; Krishnamurty, M.; Petroff, P.; Firouzi, A.; Janicke, M.; Chmelka, B. F. *Science* **1993**, *261*, 1299.
(6) Huo, Q.; Leon, R.; Petroff, P. M.; Stucky, G. D. *Science* **1995**, *268*, 1324.
(7) Huo, Q.; Margolese, D. I.; Stucky, G. D. *Chem. Mater.* **1996**, *8*, 1147.
(8) Zhao, D.; Huo, Q.; Feng, J.; Kim, J.; Han, Y.; Stucky, G. D. *Chem. Mater.* **1999**, *11*, 2668.
(9) Zhao, D.; Huo, Q.; Feng, J.; Chmelka, B. F.; Stucky, G. D. *J. Am. Chem. Soc.* **1998**, *120*, 6024.
(10) Tanev, P. T.; Pinnavaia, T. J. *Science* **1995**, *267*, 865.
(11) Bagshaw, S. A.; Prouzet, E.; Pinnavaia, T. J. *Science* **1995**, *269*, 1242.
(12) Kim, S. S.; Zheng, W.; Pinnavaia, T. J. *Science* **1998**, *282*, 1302.
(13) Kimura, T.; Kamata, T.; Fuziwara, M.; Takano, Y.; Kaneda, M.; Sakamoto, Y.; Terasaki, O.; Sugahara, Y.; Kuroda, K. *Angew. Chem., Int. Ed.* **2000**, *39*, 3855.

10.1021/cm0116929 CCC: $22.00
Published on Web 05/01/2002

nal, cubic (bicontinuous phases), random bicontinuous (spongelike), and lamellar.[14] In addition, other phases, intermediate between the hexagonal and lamellar phases, are sometimes detected.[15−17]In practice, ribbon-intermediate phases (with rectangular or monoclinic symmetry) coexist in thermal equilibrium with the normal hexagonal phase, and they may be regarded as distorted forms of the hexagonal phase in which the cylindrical micelles are flattened.[17,18] Temperature and concentration domains corresponding to ribbon-intermediate phases are usually very narrow, which is the reason they have frequently gone unnoticed or are really difficult to detect. Difficulties increase when such a system gets complicated by the addition of new components (inorganic salts, cosolvents, or cosurfactants), not to mention the effects of the new variables (pH, kinetic parameters) that the hydrolysis and condensation chemistry of an inorganic phase introduces. Hence, an accurate knowledge of the mesophase map of a given pure organic phase−water system may be a priori a useful guide to synthesize mesoporous solids, but such phase diagrams only can be considered as rough guides. In fact, the SBA-8 mesophase constitutes the only known mesoporous silica having an intermediate ribbonlike organization. It was first synthesized by Stucky and co-workers, who used bolaforms as structural directing agents.[8] Like the related gemini surfactants, bolaforms have rigid molecules including two hydrophilic headgroups connected by a hydrophobic chain (i.e., they are amphiphiles). A collateral problem in relation to these surfactants is that they are not commercial reagents, so specific preparation and purification procedures are required.

As an alternative way, in this work we describe a simple two-step route for obtaining the SBA-8 mesoporous silica. By using silatrane derivatives (complexes containing triethanolamine-like ligands) as the silicon source, we have been able to satisfactorily replace bolaforms by commercial cetyltrimethylammonim bromide (CTMABr), which currently is the surfactant most widely utilized in the synthesis of ordered mesostructured/mesoporous materials. Also, by controlling fundamental parameters (like reaction time and temperature), it becomes possible to modulate the resulting material topology.

Experimental Section

Synthesis. The method is based on the use of a cationic surfactant (CTMABr) as the supramolecular template (and, consequently, as a porogen after template removal) and a complexing polyalcohol (2,2′,2″-nitrilotriethanol or triethanolamine, $N(CH_2-CH_2-OH)_3$, hereinafter TEAH3) to favor the hydrolytic processes generating the silicon-containing moieties which condense on the surfactant headgroups.[19−21]

Chemicals. All reagents [CTMABr, tetraethyl orthosilicate (TEOS), TEAH3, and NaOH] were used as-received from Aldrich.

Synthesis of SBA-8. In a typical synthesis leading to the SBA-8 mesophase, 0.51 g of NaOH (0.0123 mol) were dissolved at 50−60 °C in a TEAH3 (23 mL, 0.173 mol) solution containing 0.049 mol of silatrane derivatives of TEAH3 (e.g., in the form of Si(TEA)OR, R = $CH_3CH_2O^-$ or $TEAH_2^-$; they can be prepared as described in the literature)[19−23] and 4.23 g of CTMABr (0.0116 mol). Then, 80 mL (4.44 mol) of water were added with vigorous stirring at a mixing temperature of 110 °C. Thus, the molar composition of the starting reagent mixture was 1:3.5:0.25:0.25:90 Si:TEAH3:NaOH:CTAMBr:H_2O. This solution was allowed to cool at room temperature (20 °C), which resulted in the formation of a white mesostructured solid. In a second step, this mixture was hydrothermally aged at 120 °C for 2 days (longer reaction times, up to 6 days, were also tested) to favor the mesostructure stabilization. After aging, the solid was filtered off, washed with water and ethanol, and air-dried. Finally, to obtain the mesoporous SBA-8 material, the surfactant was removed by calcination at 550 °C for 7 h under a static air atmosphere.

Synthesis of MCM-41. This well-known mesophase was prepared almost exactly as described above for SBA-8, the only procedural modifications being the mixing temperature and aging conditions. In a typical synthesis, we started from a solution containing exactly the same reagent amounts (0.51 g of NaOH (0.0123 mol), 23 mL of TEAH3 (0.173 mol), 0.049 mol of silatrane, and 4.23 g of CTMABr (0.0116 mol)) as those above. Then, 80 mL (4.44 mol) of water was added with vigorous stirring at a mixing temperature of 50 °C, and the resulting solution was allowed to cool at room temperature (20 °C), which also resulted in the formation of a white mesostructured solid. Instead of subjecting it to hydrothermal treatment, this mixture was aged at room temperature (20 °C) while being stirred for 3 h. Then, the solid was filtered off, washed with water and ethanol, and air-dried. Finally, to obtain the mesoporous MCM-41 material, the surfactant was removed by calcination at 550 °C for 7 h under a static air atmosphere.

Characterization

Surfactant and TEAH3 contents in the mesostructured solids were determined by CNH elemental analysis. X-ray powder diffraction (XRD) data were recorded on a Seifert 3000TT $\theta-\theta$ diffractometer using Cu Kα radiation. Patterns were collected in steps of 0.02°(2θ) over the angular range 1−10°(2θ) for 25 s/step. Electron microscopy study (TEM micrographs and electron diffraction patterns) was carried out with a Hitachi H9000NAR electron microscope operating at 300 kV, giving a point-to-point resolution of 0.18 nm. Samples were gently ground in butanol, and microcrystals were deposited on a holey carbon film supported on a Cu grid. Surface area and pore size values were calculated from nitrogen adsorption−desorption isotherms (−196 °C) recorded on a Micromeritics ASAP-2010 automated instrument. Calcined samples were degassed at 130 °C for 10 h prior to analysis. Surface areas were estimated according to the BET model, and pore size dimensions were calculated by using the BJH method. ^{29}Si MAS NMR spectra were recorded on a Varian Unity 300 spectrometer operating at 79.5 MHz and using a magic angle spinning speed of at least 4.0 kHz.

Results and Discussion

Synthesis Strategy. The previously described synthetic route for obtaining the SBA-8 mesoporous silica

(14) Fontell, K. *Colloid. Polym. Sci.* **1990**, *268*, 264.
(15) Pilsl, H.; Hoffmann, H.; Hoffmann, S.; Kalus, J.; Kenkono, A. W.; Lindner, P.; Ulbricht, W. *J. Phys. Chem.* **1993**, *97*, 2745.
(16) Hagslatt, H.; Soderman, O.; Jonsson, B. *Liquid Cryst.* **1994**, *17*, 157.
(17) Hagslatt, H.; Soderman, O.; Jonsson, B. *Liquid Cryst.* **1994**, *12*, 667.
(18) Vargas, R.; Mariani, O.; Gulik, A.; Luzzati, V. *J. Mol. Biol.* **1992**, *225*, 137.
(19) Cabrera, S.; El Haskouri, J.; Guillem, C.; Latorre, J.; Beltrán, A.; Beltrán, D.; Marcos, M. D.; Amorós, P. *Solid State Sciences* **2000**, *2*, 405.
(20) El Haskouri, J.; Cabrera, S.; Caldés, M.; Alamo, J.; Beltrán, A.; Marcos, M. D.; Amorós, P.; Beltrán, D. *Int. J. Inorg. Mater.* **2001**, *3*, 1157.
(21) Amorós, P.; Beltrán, A.; Beltrán, D.; Cabrera, S.; El Haskouri, J.; Marcos, M. D. Patent WO 01-72635, 2000.
(22) Frye, C.; Vicent, G.; Finzel, W. *J. Am. Chem. Soc.* **1971**, *93*, 6805.
(23) Verkade, J. G. *Acc. Chem. Res.* **1993**, *32*, 2711 and references therein.

is based on the control of the symmetry of the final material by the organic counterpart.[8] Thus, this phase was synthesized by using rigid bolaform surfactants {specifically $[(CH_3)_3N^+(CH_2)_{12}-O-C_6H_4-C_6H_4-O-(CH_2)_{12}-N^+(CH_3)_3](Br^-)_2$} as templates. Both theoretical and experimental studies indicate that this type of amphiphiles present an aggregation behavior more specific than conventional surfactants having flexible hydrophobic chains.[24] Hence, the proper steric constrains of these rigid templates could account for the characteristic anisotropy of the SBA-8 phase. In practice, this is a polished successfully synthetic approach. However, besides its apparent singularity, such a synthetic strategy requires previous somewhat cumbersome processes of preparation and purification of the template agents.[25]

The alternative strategy now reported involves two main procedural features, namely, the use of silatrane complexes as the source of Si reactive species and the use of a conventional (and commercial) alkyltrimethylammonium surfactant (CTMABr) as a template. It must be remarked that silatrane solutions are easily and quickly prepared without additional purification or crystallization steps.[19−23] On the other hand, it is the adequate control of kinetic parameters which finally makes it possible to modulate the topology of the resulting material, that is to say, to obtain the characteristic anisotropy of the SBA-8 mesophase. In practice, we are simply playing with (1) the temperature (T_m), at which occur the hydrolytic and subsequent condensation processes involving the silatrane complexes, processes that give rise to the inorganic portions which must fit together with the surfactant micelles and (2) the aging conditions (temperature, T_a, and time, t). It is also important in this context to emphasize that such kinetic factors affect the reactivity of both the inorganic and organic species involved in the self-assembling processes.

Dealing with CTMABr, it is well-known that polar organic species (such as ethanol, $(CH_3)_2NCH_2CH_2OH$, and TEAH3) penetrate the hydrophobic and palisade regions of micelles and thereby induce structural rearrangements of the surfactant phase (that should affect both the micelle geometry and its charge density at the interface).[7] The relatively high mixing temperature we have used in this work intensifies the mobility of the nonrigid surfactant molecules and changes the effect of cosolvent organic species, this favoring the incorporation of TEAH3 molecules in the $CTMA^+$ aggregates. Therefore, the participation of TEAH3 molecules in the organic aggregates should be responsible for the template distortion to obtain elliptically shaped micelles. This type of distortion leading to the anisotropic rectangular *cmm* symmetry has been previously characterized in surfactant−water systems (CTMABr−water and SDS−water).[26−28]

On the other hand, the relatively high T_m value (the hydrolysis occurred at room temperature in the previously reported synthesis of SBA-8)[8] also favors the stabilization of the *cmm* rectangular phase in that depending on the silatrane precursors reactivity. After water addition, the most outstanding feature concerning the hydrolytic reactivity of silatrane complexes (when compared to TEOS) is their lability.[19,20,29] Thus, the majority of silatrane species (which in an anhydrous medium in the presence of NaOH is $SiNa(TEA)_2H_2^+$, according to FAB-MASS data analysis in previous works) presents hydrolysis and condensation reaction rates higher than conventional alkoxides (such as TEOS), this favoring the formation of Si−O−Si bonds.[19,29] This last is consistent with the results of ^{29}Si NMR experiments (see below), which show that there is a low proportion of Q^3 silicon environments in the mesostructure. In fact, this observation seems to be general (independent of the specific composition and/or final pore topology) in the case of silica-based mesoporous solids prepared through the atrane route.[19,29,30] Thus, the MCM-41 phase synthesized from atrane precursors also has a Q^3/Q^4 ratio lower than that usually observed when this material is prepared from TEOS. Indeed, in most of the reported syntheses, it is said that hydrothermal treatments near 100 °C are required to stabilize the hexagonal ordered MCM-41 mesostructured phase.[31] On the other hand, the silica condensation degree increases with temperature. Thus, both factors (the enhanced reactivity of the silatrane complexes and the relatively high mixing temperature) work together to produce a rapid silica polymerization that quickly locks the distorted structure in place.

The as-synthesized SBA-8 mesostructured material (prior to hydrothermal treatment) shows poor crystallinity. This notwithstanding, its XRD pattern displays an intense peak together with a shoulder in the low-angle region that can be indexed (taking into account the subsequent hydrothermal evolution) to the (110) and (200) reflections of the rectangular cell. The low-intensity peaks typical of the SBA-8 phase are not detected prior to the aging treatment. The postsynthesis hydrothermal treatment at 120 °C simply increases the phase crystallinity, as measured by the enhanced resolution of the XRD peaks. Now, the patterns include both the (110) and (200) intense peaks together with, at least, five additional peaks of low intensity. Only slight differences are detected by prolonging the aging time from 2 to 6 days (Figure 1).

Our results show that both the SBA-8 and MCM-41 mesostructured/mesoporous silicas can be prepared with the cooperation of the relatively small and soft CTMABr surfactant. It is interesting, however, that the relative temperature conditions in our experiments are reversed with respect to those reported in the synthesis using bolaform surfactants.[8] In this last case, the mesostructured SBA-8 material, which is obtained at room temperature, evolves toward the MCM-41 silica by gently heating it in water or in the mother liquor.[8] When prepared through the atrane route, all occurs as if the low- and high-temperature phases were the MCM-41

(24) Taylor, M. P.; Herzfeld, J. *Langmuir* **1990**, *6*, 911.
(25) Kunitabe, T.; Okahata, Y.; Shimomura, M.; Yasunami, S.; Takarabe, K. *J. Am. Chem. Soc.* **1981**, *103*, 5401.
(26) Laughlin, R. G. *The Aqueous Phase Behavior of Surfactants*; Academic Press: San Diego, 1994; p 215.
(27) Kekicheff, P.; Cabane, B. *J. Phys.* **1987**, *48*, 1571.
(28) Rendall, K.; Tiddy, G. J. T.; Trevethan, M. A. *J. Chem. Soc., Faraday Trans. 1* **1983**, *79*, 637.
(29) El Haskouri, J.; Cabrera, S.; Gutierrez, M.; Beltrán, A.; Beltrán, D.; Marcos, M. D.; Amorós, P. *Chem. Commun.* **2001**, 309.
(30) Cabrera, S.; El Haskouri, J.; Mendioroz, S.; Guillem, C.; Latorre, J.; Beltrán, A.; Beltrán, D.; Marcos, M. D.; Amorós, P. *Chem. Commun.* **1999**, 1679.
(31) Corma, A. *Chem. Rev.* **1997**, *97*, 2373 and references therein.

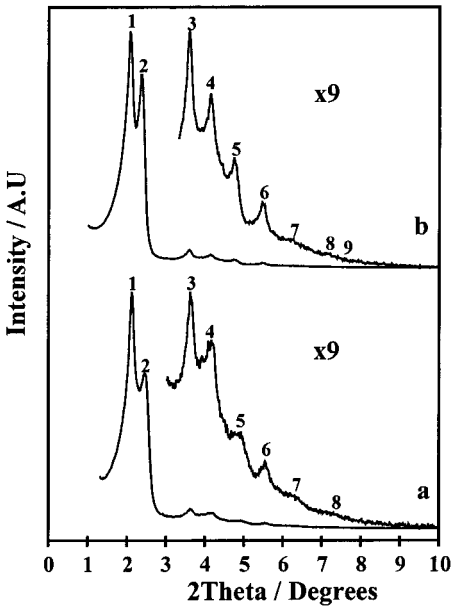

Figure 1. XRD patterns of SBA-8 mesostructured materials synthesized at different aging times (t). (a) $t = 2$ days. (b) $t = 6$ days.

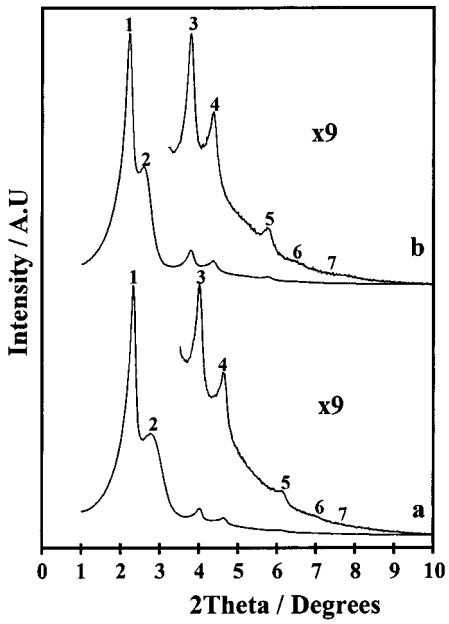

Figure 2. XRD patterns of SBA-8 calcined mesoporous materials synthesized at different aging times (t). (a) $t = 2$ days. (b) $t = 6$ days.

($T_m = 50$ °C; $T_a = 20$ °C) and SBA-8 ($T_m = 110$ °C; $T_a = 120$ °C) phases, respectively. Once formed, hydrothermal treatment (at $T_a = 100-120$ °C) of any of these phases only results in a better XRD pattern definition, and no phase transformation is detected. A priori, these results might seem striking. However, as indicated above, there is a clear dependence with temperature of the two key factors in our preparation, namely, the acceleration of the silica condensation induced by the use of silatranes and, mainly, the incorporation of TEAH3 into the $CTMA^+$ micelles (which result in distortion). Cooperative self-assembling of highly condensed silicon moieties with the more cylindrical (low temperature) or flattened (high temperature) organic aggregates should lead to the immediate stabilization of MCM-41 or SBA-8 mesophases, respectively.

Characterization. The fact that TEAH3 enters the supramolecular template is clearly shown by the CNH elemental analysis of the mesostructured materials. In practice, the experimental value of the C/N weight ratio in the MCM-41 mesophase (16.15) is still very close to the nominal one corresponding to CTMABr (16.28). However, the C/N value decreases (15.03) in the SBA-8 mesostructured solid, a value which is consistent with the incorporation of a significant amount of TEAH3 molecules (≈10%) to the organic template.

The XRD patterns of representative samples of the mesostructured (after postsynthesis hydrothermal treatment) and mesoporous (calcined and aged) SBA-8 materials are shown in Figures 1 and 2, respectively. As can be noted, all the samples display very similar patterns: two intense and partially overlapped peaks at low-angle values (≈38−39 Å), and some other weaker features at higher 2θ values (which, in some cases, appear rather well-resolved in five to six diffraction peaks). These patterns have been indexed (by using the LSUCRE program) with two-dimensional rectangular cells (*cmm* symmetry, see Table 1), which are similar to those proposed for the SBA-8 silicas by Stucky and co-workers.[8] Despite their similarity, the patterns in Figures 1 and 2 show a certain evolution that is dependent on both the aging time and the nature of the mesophase (mesostructured or mesoporous). Indeed, the patterns of the mesostructured phases (Figure 1) clearly present a resolution higher than those corresponding to the respective final mesoporous (calcined) materials (Figure 2). Also, when the postsynthesis hydrothermal treatment is prolonged (from 2 to 6 days), a certain increase in the phase crystallinity is achieved for both the mesostructured and mesoporous materials. On the other hand, with the cell parameter values (see Table 1), it can be noted how the surfactant removal (as a consequence of calcination) completes the condensation of the silica framework, which is reflected by the cell shrinkage. As could be expected, the cell contraction in the case of the SBA-8 materials described here (≈9%) is, however, significantly lower than that reported in ref 8 (20%). A similar cell contraction value (≈10%) is observed for the mesostructured to mesoporous transition of the MCM-41 phase prepared through the atrane route. This result is consistent with the already mentioned raised polymerization associated with our synthetic approach. In addition, the cell dimensions increase with the time of the hydrothermal treatment. We will return to this point later on.

Transmission electron microscopy (TEM) images and electron diffraction patterns fully correlate with XRD observations. The TEM micrographs and electron diffraction patterns in Figure 3 correspond to a representative sample of the calcined SBA-8 material (hydrothermally aged for 2 days). Both the typical distorted hexagonal array (Figure 3a, [10] zone plane) and the cylinder packing (Figure 3b, [11] zone plane) are clearly shown. We can see that the mesoporous SBA-8 solid prepared through the atrane route effectively has a highly ordered bidimensional array with centered rectangular (*cmm*) symmetry.

The SBA-8 mesophases can be considered as distorted forms of the ordered hexagonal MCM-41 (*p6mm*) ones.

Table 1. Indexation of the XRD Patterns of Mesostructured and Mesoporous SBA-8 Silicas Synthesized by the Atrane Route

	mesostructured SBA-8				mesoporous SBA-8			
		$t = 2$ days[a]		$t = 6$ days[b]		$t = 2$ days[c]		$t = 6$ days[d]
hkl	peak (no.)[e]	(d/Å)	peak (no.)[e]	(d/Å)	peak (no.)[e]	(d/Å)	peak (no.)[e]	(d/Å)
110	1	41.70	1	42.44	1	38.05	1	39.76
200	2	35.00	2	37.40	2	32.00	2	33.95
020	3	24.90	3	24.52	3	21.96	3	23.23
310	4	21.22	4	21.22	4	19.02	4	20.15
400	5	18.07	5	18.62				
130	6	15.94	6	16.11	5	14.43	5	15.27
420	7	14.30	7	14.10	6	12.80	6	13.67
430	8	12.10	8	12.40	7	11.00	7	11.41
240			9	11.94				

[a] $a = 70.4(8)$ Å, $b = 49.4(3)$ Å. [b] $a = 74.9(9)$ Å, $b = 49.8(5)$ Å. [c] $a = 64.6(9)$ Å, $b = 44.8(8)$ Å. [d] $a = 67.5(9)$ Å, $b = 46.8(7)$ Å. [e] Peak numbers according to Figures 1 and 2.

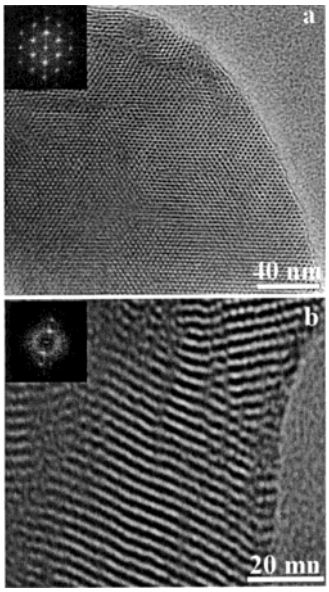

Figure 3. TEM micrographs and electron diffraction patterns (inset) of mesoporous SBA-8 silica along (a) the (100) and (b) (110) directions.

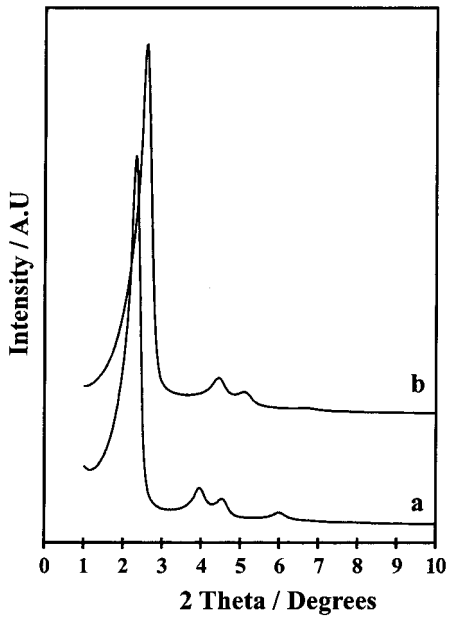

Figure 4. XRD patterns of (a) mesostructured and (b) mesoporous MCM-41 silicas synthesized by the atrane method.

The distortion can be thought of as consisting of a simultaneous shrinkage and elongation of the cell along the (100) and (010) directions, respectively. Indeed, we have calculated the cell parameters corresponding to the MCM-41 materials synthesized as described in this work (see Figure 4). Assuming a centered rectangular cell (for comparison), these values are $a = 76.2(8)$ Å, $b = 43.9(6)$ Å (mesostructured MCM-41), and $a = 67.9(8)$ Å, $b = 39.2(5)$ Å (mesoporous MCM-41). When compared to the respective values calculated for the SBA-8 phases (Table 1), the above-mentioned MCM-41/SBA-8 relation seems clear. In this context, the distortion of the hexagonal cell can be quantified in terms of the a/b ratio. As it could not be any other way, this value exactly is $\sqrt{3}$ for MCM-41, and lower or higher values could be found for the SBA-8 phases. In our case, the distortion in the lattice of the SBA-8 mesoporous material results in an a/b ratio of 1.44 ($a/b < \sqrt{3}$), which is slightly lower than that previously reported in ref 8 ($a/b = 1.50$). Taking as reference the intermediate mesophases detected in pure surfactant−water systems, it must be said that there is no reported evidence about the existence of any *cmm* lyotropic liquid-crystal-like mesophase for which $a/b < \sqrt{3}$. In contrast, rectangular distortions of the hexagonal cell in the opposite sense ($a/b > \sqrt{3}$) have been observed in surfactant−water binary systems (such as sodium dodecyl sulfate−water, $a/b = 2.2-2.8$)[8,26,27] and also in mesostructured silicas (Stucky and co-workers referred to a M_α silicate phase with $a/b = 2.06$).[8] Thus, the SBA-8 mesoporous material, as occurs in the case of the SBA-2 silica, does not seem to have a lyotropic liquid-crystal-like mesophase surfactant counterpart.[6]

Mesoporosity of the SBA-8 material is further illustrated by the N_2 adsorption−desorption isotherms (Figure 5). Regardless of the aging time ($t = 2$ or 6 days), the curves show one well-defined step characteristic of Type IV isotherms, which should be due to capillary condensation of nitrogen inside the mesopores. The absence of significant hysteresis loops, as well as their sharp curvature, confirm the existence of an unimodal and narrow pore size distribution, this indicating good quality of the final material. In any case, by prolonging the postsynthesis hydrothermal treatment (from 2 to 6 days), we can detect a slight increase of both the BET surface area (from 944 to 1022 m^2/g) and the BJH pore size (from 26.5 to 29.1 Å). The averaged values of the pore wall thickness (≈21.7 Å ($t = 2$ days) and 20.8 Å ($t = 6$ days)), estimated from porosity and XRD data, are similar to those observed in other silica-based meso-

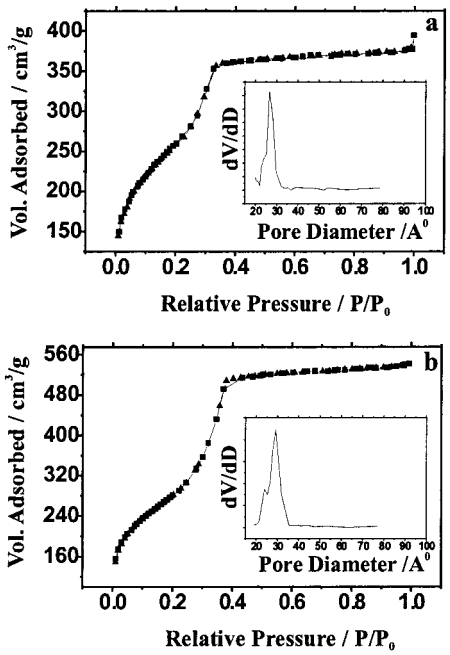

Figure 5. N_2 adsorption−desorption isotherms and pore size distributions (inset) of SBA-8 silicas synthesized with different aging times (t). (a) $t = 2$ days. (b) $t = 6$ days.

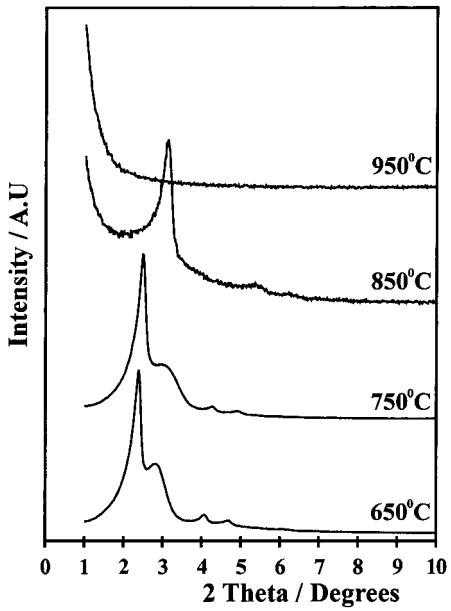

Figure 6. Evolution of the XRD patterns of SBA-8 silica as the temperature increases.

porous materials prepared from the atrane route,[19−21,29,30] and higher than those reported in previous works referred to MCM-41 silicas.[31] In practice, the calculated pore size and wall thickness values must be considered with caution because of problems related to using the BJH method. Notwithstanding, dealing with MCM-41-related materials, BJH values are useful for comparative purposes (given that this standard method systematically underestimates the pore diameter and subsequently overestimates the pore wall thickness by ca. 0.7−1.0 nm).[32−34] Taking into account that the pore wall thickness remains practically unchanged (at least for aging periods such as those reported here), the cell expansion detected by XRD should be basically related to pore size variations. In fact, the cell parameter expansion (2.5 Å, measured as the average of the changes along the (100) and (010) directions) with the aging time (from 2 to 6 days) fits in very well with the BJH pore size variations (2.6 Å). This fact might be tentatively attributed to the entering of a higher amount of TEAH3 molecules into the $CTMA^+$ micelles, which should be favored by prolonging the reaction time at a relatively high temperature.

On the other hand, with regard to MCM-41-related silicas, it has been previously argued on how the pore wall thickness correlates to the stability of mesoporous materials.[35,36] In our case, taking into account the intermediate-distorted nature of the SBA-8 mesoporous phase, it does not seem excessive to state that it possesses significant thermal stability, as measured by the permanence ot its X-ray diffraction peaks at 750 °C. Indeed, shown in Figure 6 is the temperature dependence of the XRD pattern of a representative sample of the SBA-8 mesophase. In practice, we have subjected the sample to successive thermal treatments, while maintaining the temperature of treatment for periods of 7 h. When the temperature is heated from room temperature up to 750 °C, the pattern evolution is similar to that observed in the case of other MCM-41-like mesoporous solids. Thus, we can observe (1) a small contraction of the cell, which probably is associated with the condensation of some remaining silanol groups and (2) an increase of the fwhm of the reflections with temperature (the peaks resolution decreases). However, up to 750 °C, the XRD pattern maintains the intense (110) and (200) reflections together with, at least, three additional low-intensity peaks, which corresponds to the rectangular cell of the SBA-8 mesoporous material. The mesostructure collapses at 950 °C, but a solid-state phase transition from SBA-8 to MCM-41 is detected prior to such a collapse. This high-temperature MCM-41 phase (850 °C) displays a contracted cell ($a_0 = 33.95$ Å, considering the typical hexagonal cell). In fact, this is a usual solid-state evolution from low (cmm) to high ($p6mm$) symmetry as the temperature increases. Insofar as our synthesis conditions are relatively soft (in comparison with previous reports in the literature),[35] the mesostructure collapse temperature (950 °C) is relatively high, which should be related to a high condensation level in the thick pore silica walls.

The high level of polymerization of the silica walls can be tested through ^{29}Si MAS NMR, both in mesostructured and mesoporous SBA-8 materials (Figure 7). The relative concentration of Q^3 silicon environments is very low, even in the mesostructured (noncalcined) SBA-8 materials. The spectra of these solids present an intense signal centered at ca. $\delta = -108-109$ ppm and a smaller one at ca. $\delta = -98-99$ ppm, which can be assigned to Q^4 [Si(4Si)] and Q^3 [Si(3Si, OH] silicon sites, respectively. Deconvolution of these spectra lead to a small Q^3/Q^4 ratio (0.8 and 0.6 for solids hydrothermally treated for 2 and 6 days, respectively). As expected, after

(32) Kruk, M.; Jaroniec, M.; Sayari, A. *J. Phys. Chem. B* **1997**, *101*, 583.
(33) Sonwane, C. G.; Bhatia, S. K. *J. Phys. Chem. B* **2000**, *104*, 9099.
(34) Ravikovitch, P. I.; Wei, D.; Chueh, W. T.; Haller, G. L.; Neimark, A. V. *J. Phys. Chem. B* **1997**, *101*, 3671.
(35) Mokaya, R. *J. Phys. Chem. B* **1999**, *103*, 10204.
(36) Chen, L.; Horiuchi, T.; Mori, T.; Maeda, K. J. *Phys. Chem. B* **1999**, *103*, 1216.

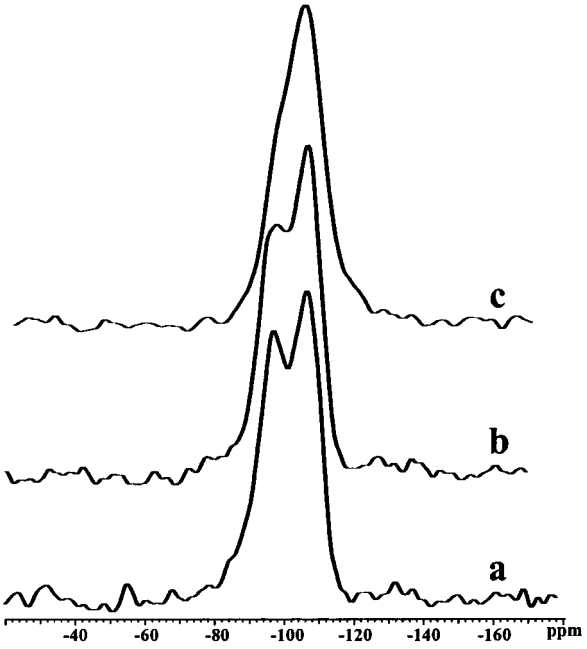

Figure 7. ^{29}Si MAS NMR spectra of (a) mesostructured (2 days of hydrothermal treatment), (b) mesostructured (6 days of hydrothermal treatment), and (c) mesoporous SBA-8 silica.

thermal treatment (T = 550 °C, 7 h), the amount of silanol groups is still very much lower than that in the as-synthesized material. The ^{29}Si MAS NMR spectrum of the mesoporous SBA-8 material displays one intense signal centered at $\delta = -110-112$ ppm and a small shoulder at lower chemical shift, ca. −100 ppm (typical of high condensed silica networks). Numerical deconvolution indicates that the Q^3/Q^4 ratio is extremely low (0.24). We have found similar Q^3/Q^4 ratio values in the cases of MCM-41, MCM-48, and other substituted silicas synthesized through the atrane route.[19,20,29,30] On the other hand, as far as we know, other similar Q^3/Q^4 ratios in related mesoporous silicas have been achieved after vigorous synthesis conditions or postsynthesis treatments specifically addressed to improve the thermal stability of the silicas.[35,36] As previously mentioned, the NMR experiments confirm in this way the high degree of condensation achieved when combining relatively high reaction temperatures (T_m) and the use of reactive silatrane complexes as the Si source, both being factors which are responsible for the SBA-8 stabilization.

Concluding Remarks

Missing a phase is a general problem in phase research and particularly severe during studies of surfactant systems. Difficulties increase when thinking about intermediate phases that only can be detected under a very narrow set of conditions, even more if a new phase (such as silica) is included in the phase map. From the above, it seems evident that with regard to the preparation of mesostructured/mesoporous materials, procedural variables define a very complex system in which kinetic parameters (reaction time, basic operations sequence) can play a determinant role. In other words, we clearly are involved in the design of "*nonabelian*" synthetic strategies. Hence, the synthesis space diagram for obtaining mesoporous materials includes a versatile set of variables such as relative concentration and nature of the reagents, pH, temperature, and reaction time. While the previously reported synthesis of the SBA-8 silica is based on specific template effects, our strategy, without prejudice from the template effect derived from the incorporation of TEAH3 in the micelles, is based on careful control of the kinetic parameters affecting the hydrolysis and condensation of the inorganic species.

Acknowledgment. We thank the Spanish Ministerio de Ciencia y Tecnología (Grants PB98-1424-C02-01 and MAT2000-1387-C02-01) and the Agencia Española de Cooperación Internacional for financial support.

CM0116929